doi.org/10.36721/PJPS.2026.39.6.174.1

Development of oral piperaquine nanoparticles: A study on formulation, characterization and *in-vivo* performance

Seema Bakht[1], Jahangir Khan[1*#], Maqsood Ur Rehman[1*#], Muhammad Asif Khan[2], Aziz-Ur-Rahman[1], Imran Tariq[3], Haya Hussain[4], Shujaat Ahmad[4] and Rukhsana Ghaffar[1]

[1]Department of Pharmacy, University of Malakand, Chakdara, Pakistan
[2]Department of Pharmacy, Sarhad University of Science & IT, Peshawar, Pakistan
[3]Punjab University College of Pharmacy, University of the Punjab, Lahore, Pakistan
[4]Department of Pharmacy, Shaheed Benazir Bhutto University Sheringal Dir (Upper), Pakistan

Abstract: **Background**: Piperaquine (PQ) is an anti-malarial bisquinoline BCS Class-II drug having low aqueous solubility and oral bioavailability, which affects its therapeutic effectiveness. Pharmaceutical Nanotechnology has proved its potential to overcome the challenges associated with poorly water-soluble drugs. **Objectives**: The fabrication of Piperaquine nanoparticles (PQ-NPs) through the antisolvent technique with subsequent characterization to improve the dissolution and bioavailability was the primary objective. **Methods**: PQ-NPs were prepared using anti-solvent precipitation Method. The polymers hydroxypropyl methylcellulose (HPMC) of 0.25%, polyvinylpyrrolidone (PVP-K30) of 0.25 %, and sodium lauryl sulfate (SLS) of 0.5 % were used as stabilizers. The Particle size, PDI, zetapotential, DSC, XRD, SEM, In-vitro dissolution, and in vivo study were performed for characterization of PQ-NPs. **Results**: The produced optimized PQ-NPs had a particle size of 184 nm, PDI of 0.248 and zeta potential of -31.4 mV. The NPs had a lower melting point and crystalline content, as shown by differential scanning calorimetry (DSC) and XRD. The SEM analysis confirmed the smaller particle size with a larger surface area. PQ-NPs showed a significantly faster release profile than raw drug, achieving 79.56% drug release in 5 minutes versus 27.31% ($p < 0.05$). Pharmacokinetic studies in mice revealed that C_{max},T_{max} and AUC were significantly enhanced for PQ-NPs (C_{max}: 2.753 µg/ml vs. 1.233 µg/ml; T_{max}: 1.0 ± 0.3 hr vs 1.5 ± 0.3 hr, AUC: 1.119 µg.hr/ml vs. 0.954 µg.hr/ml. **Conclusion**: The findings indicate that PQ-NP were successfully fabricated, having substantial improvements in solubility, dissolution rate, and bioavailability, making them a promising approach for enhancing the therapeutic performance.

Keywords: Anti-solvent precipitation; Bioavailability; Dissolution rate; Nanoparticles; Piperaquine

Submitted on 07-05-2025 – Revised on 07-08-2025 – Accepted on 11-08-2025

INTRODUCTION

Nanotechnology has emerged as a transformative platform in pharmaceutical research, particularly for improving the delivery of poorly water-soluble drugs and has garnered a lot of interest over the past few decades(Mitchell *et al*., 2021). One of the major contributions of nanoparticles (NPs) in pharmaceutical field is the advantage that might be achieved by fabricating drugs with limited solubility (Mitchell *et al*., 2021; Dolatabadi *et al*., 2021; KumarDalvi and Siril, 2020; Da Silva *et al*., 2020). Nanoparticles of a drug are nano-scale particles measuring 1-1000 nm (Ran *et al*., 2022). Encapsulating molecules of drug by employing nanotechnology offers several benefits over the traditional dosage form, including higher efficiency of encapsulation, sustained and controlled release, targeted delivery and enhanced bioavailability (Hami, 2021). Theoretical guidelines presented by the Noyes-Whitney and Ostwald-Freundlich equations demonstrate that reducing size of particle could result in enhanced solubility and dissolution kinetics. As a result, nanosizing has become a widely adopted strategy for formulating Biopharmaceutics Classification System (BCS) Class II and IV drugs, which are characterized by limited aqueous solubility (Sabra *et al*., 2024). Various techniques, including both top-down, such as the emulsification method (Parida *et al*., 2024), high-pressure homogenization and the ball milling method (Bhalani *et al*., 2022) and bottom-up, such as the anti-solvent precipitation technique and the supercritical anti-solvent precipitation technique (Zhang *et al*., 2024), have been employed to prepare drug nanoparticles. Amongst these techniques, the antisolvent precipitation technique is the most cost-effective and efficient technique for developing nano-functional components (Song *et al*., 2025). The antisolvent precipitation technique is being effectively used to produce nanoparticles of certain drugs, including Dexibuprofen, indomethacin and ketoprofen (Kumar *et al*., 2023).Oral administration of drugs remains the most convenient and patient compliant route of drug delivery, as it offers physiological advantages, as the GI tract provides a larger surface area for the absorption of drug. However, many therapeutic agents suffer from poor absorption owing to low solubility and permeability in the gastrointestinal (GI) environment. Therefore, developing

*Corresponding author: e-mail: jahangirkhan222@gmail.com, mrehman@uom.edu.pk
#These authors contributed equally and are the co-first authors.

advanced oral delivery systems such as drug nanocrystals is critical to overcoming these limitations and improving therapeutic outcomes (Alqahtani *et al*., 2021). For that reason, there is a growing interest in developing effective drug delivery systems, which can effectively overcome biological challenges and enhance oral bioavailability (Lou *et al*., 2023).

The PQ is a synthetic 4-aminoquinoline derivative of dihydroartemisinin, has a chemical structure of 1,3-bis[4-(7-chloroquinolinyl-4)piperazinyl-1]propane (C29H32Cl2N6) (Fonte *et al*., 2021) and exhibits strong blood schizonticidal activity (SharmaAgarwal and Awasthi, 2023)preferred for antimalarial treatment due to its superior compliance and efficacy, resulting in the distribution of over 140 million therapeutic dosages for adults (Mishra *et al*., 2021). Therefore, this study aims to develop and optimize nanocrystal formulations of PQ for enhancing its bioavailability and therapeutic effectiveness.

MATERIALS AND METHODS

PQ was acquired from Shaanxi DideuMedichem Co, Ltd, China, Polyvinylpyrrolidon (PVP-K30), hydroxypropyl methylcellulose (HPMC), sodium lauryl sulphate (SLS), Eudragit S-100, Polyethylene glycol (PEG-4000) and Chloroform of Sigma Aldrich were gifted by the Z-Jans Pharma, Peshawar, Pakistan.

Preparation of piperaquine (PQ) NPs

An antisolvent precipitation technique was used to fabricate PQ-NPs in organic solvent. The Polymers (PVP, HPMC, PEG and Eudragit) and a surfactant (SLS) were incorporated as a stabilizer and are mentioned in table1. Hydrophilic polymers such as HPMC, PVP-K30 and Eudragit were chosen based on their ability to enhance solubility, stabilize nanoparticles and reduce drug crystallinity. SLS was used as an anionic surfactant to prevent aggregation and provide electrostatic stabilization. The concentrations of each excipient were selected based on pre-formulation screening studies and literature precedents that demonstrate optimal nanoparticle characteristics (e.g., particle size < 200 nm, low PDI) within the tested ranges. The drug-to-polymer ratios (1:9, 1:10, 1:15) were optimized based on preliminary trials to achieve desired particle size without excess excipient burden. The drug solution was prepared by adding the drug in organic solvent and properly mixed. A polymeric solution was subsequently prepared by adding polymer(s) in distilled water. These two solutions (organic and Polymeric) were mixed. The organic phase/drug solution was added dropwise to the polymeric solution (antisolvent phase) and was stirred on a magnetic stirrer at 1000 rpm for 60 minutes. The zeta sizer was used to measure the particle size and PDI of the formed NPs. The NPs were freeze-dried using a vacuum freeze dryer/lyophilizer (FDI-0950) HumanLab Inc, South Korea (Mahmood *et al*., 2023).

Optimization of PQ-NPs

A preliminary screening approach based on trial-and-error (hit-and-trial) was employed to evaluate the influence of various formulation variables, including polymer type (PEG 4000), surfactant (SLS) and drug-to-polymer ratios, on nanoparticle characteristics such as particle size and PDI. This initial screening allowed identification of promising combinations under limited experimental constraints. The antisolvent precipitation technique one factor at a time, a one-variable-at-a-time (OVAT) approach was utilized to optimize operating conditions. A systematic examination of various formulations (designated as HP1-NP to HP15-NP) was carried out to optimize the size of PQ-NPs. A different drug-to-polymer ratio, surfactant/polymer formulations and concentrations were used. It is easier to experiment with a wide range of conditions to find the best formulation for PQ's nanoparticle size. Table 1 lists the various formulations that were utilized in this study for the production of PQ-NPs.

Measurement of size of PQ-NPs

Using the Zetasizer Nano-ZS dynamic light scattering (DLS) instrument (ZS-90, Malvern Instruments, UK), the mean particle size of PQ nanoparticles was measured. A micropipette was used to measure the volume of the sample. Water served as a dispersant throughout the entire experiment. Additionally, single-use cuvettes were used for analysis, and each sample was measured in triplicate (n=3) to ensure precision. (Boscolo *et al*., 2023).

Zeta potential measurement of PQ-NPs

The measurement of zeta potential of nanosuspensions was carried out using the Zetasizer Nano-ZS instrument (ZS-90, Malvern Instruments, UK). The dilution of the samples of nanosuspensions was carried out using dispersion medium. Triplicate analysis (n=3) was performed for all samples, and the findings were stated as mean values (Boscolo *et al*., 2023).

Morphology studies

Morphology of the freeze-dried PQ-NPs and raw PQ was measured by SEM with the use of a JEOL JSM-IT 100 scanning electron microscope (Japan). The samples of raw PQ and PQ-NPs were attached to a brass base with the help of a double-sided carbon tape. Then, a thin layer of palladium and gold was used to make them conduct electricity. Finally, the SEM was set to 20KV to take images at various magnifications (Urimi *et al*., 2021).

Differential scanning calorimetry (DSC)

The phase transition of raw PQ and freeze-dried PQ-NPs was analyzed by double-furnace DSC-8000 (PerkinElmer, Inc., USA). The samples were placed in flat-bottomed aluminum pans, sealed airtight and analyzed using a differential scanning calorimeter (Diamond, PerkinElmer, USA). The temperature range scanned was 55 °C to 300 °C

at a rate of 10 °C/min, with a nitrogen gas flow rate of 20 ml/min. A blank pan was utilized for calibration and reference before each test. Glass transition temperatures, melting points and enthalpies of fusion were evaluated (GhanbariPicken and van Esch, 2023).

X-ray diffraction (XRD)

The XRD of the raw PQ and freeze-dried PQ nanoparticle was carried out using JEOL JDX-3532 X-ray diffractometer (Japan), employing a beam of Cu Ka radiation (wavelength = 1.5418 A). The samples scanning was performed at 2θ from 4-80° (step size 0.01°, scan speed 0.1 sec/step) at 25°C. XRD was performed in a symmetrical reflection mode (20-40 kV, 2.5-30 mA) (Yadav and Kumar, 2014).

Stability studies

The stability assessment of PQ nano suspensions was conducted through continuous monitoring of particle size over time at 4ºC and 25ºC. This investigation was performed to quantify particle growth due to aggregation and Ostwald ripening. Analysis of particle size was carried out on the stored samples at regular intervals of 0, 5, 10, 15, 20, 25 and 30 days using Zeta sizer (Zulbeari and Holm, 2025).

Dosage form preparation

The PQ-NPs were mixed with excipients, 1% talc and 0.5% HPMC, while the raw drug was used in its pure form. Each of the six capsules was filled with 160 mg of PQ-NPs and 2.4 mg of excipients. Similarly, each of the six capsules was filled with 160 mg of raw PQ. The tests were performed in triplicate (Zhang *et al*., 2024, Bhalani *et al*., 2022).

Dissolution studies

An in-vitro dissolution test was conducted on PQ-NPs and raw PQ using USP apparatus 2 (Pharmatest - PT-DT70, USA). Separate dissolution tests were conducted for PQ-NPs and raw PQ. For each test, the six capsules were placed in the dissolution apparatus vessels, with each vessel containing one capsule. The dissolution medium contained 900 mL of phosphate buffer solution, pH 7.4 and was maintained at 37°C ± 0.5°C with continuous stirring at 75 rpm, as reported for nanosuspensions. To determine PQ dissolution, 5 mL samples were taken from the dissolution bath at regular durations (5, 10, 15, 20, 25, 30, 35, 40, 45, 50, 55 and 60 minutes) using a 0.22 µm syringe filter. An equal quantity of fresh medium (phosphate buffer) was mixed to replace the collected aliquots. The samples were analyzed utilizing a UV spectrophotometer (UV-1900i Shimadzu, Kyoto, Japan) at 344 nm (HungDavis and Ilett, 2003).

Pharmacokinetic profile

Animal studies on Albino Swiss mice weighing 22.4 ± 2.2 g of both sexes were carried out. The mice were kept in a controlled environment with 12-hour cycle of light and darkness. The Albino Swiss mice were randomly assigned into two groups (raw PQ and PQ-NPs) with (n = 3). PQ-NPs were encapsulated for studies. The capsules were not administered directly to animals. For pharmacokinetic evaluation, the nanoparticle powder (equivalent to 90 mg/kg of PQ was dispersed in distilled water and the oral dose of 90 mg/kg (Haripriyaa and Suthindhiran, 2023) of PQ was administered by gavage by selecting the dilution volume of 10 ml/kg (Pandita *et al*., 2021). Plasma containing PQ was collected by drawing blood from the mice through cardiac puncture (Mollaeva *et al*., 2021, Niroumand *et al*., 2023). Pharmacokinetic parameters, including maximum concentration (C_{max}), the time to reach maximum concentration (T_{max}) and area under curve (AUC) were determined. The quantification of PQ was carried out using a previously validated HPLC method with minor modifications. Drug concentrations were measured employing a high-performance liquid chromatography (HPLC) having a series-200 LC pump and a series-200 UV/VIS detector (Perkin Elmer, USA) with following conditions: a Symmetry C18 column (100 mm × 4.6 mm, 5 µm) maintained at 25°C, with detection at 344 nm and an injection volume of 10 µL with phosphate-acetonitrile buffer(pH 2.5, 0.1 M) with a (92:8, v/v) ratio as a Mobile phase. The mixture was subsequently pumped into the HPLC equipment at a flow rate of 3 ml/min. The method complied with ICH Q2(R1) requirements and the reported LOD and LOQ were 0.05 µg/ml and 0.15 µg/ml, respectively (Graván *et al*., 2023, Khan *et al*., 2022).

Sample size and data analysis

Statistical analysis was performed using GraphPad Prism software (GraphPad Software, USA). Each experimental group consisted of n = 3 mice. Statistical analysis was performed using unpaired Student's t-test for comparing pharmacokinetic parameters between raw PQ and PQ-NP groups. A p-value < 0.05 was considered statistically significant. All data are expressed as mean ± standard deviation (SD).

RESULTS

Effect of polymer composition on nanoparticle characteristics

The study evaluated various polymers, both individually and in combination, to formulate PQ nanocrystals (PQ-NPs). The type and concentration of polymer directly influenced the particle size and polydispersity index (PDI), as summarized in fig. 1. The most favorable results were achieved with a stabilizer combination of 0.25% HPMC, 0.25% PVP-K30, and 0.5% SLS, which produced nanoparticles with a mean size of 184 nm, a PDI of 0.248, and a zeta potential of -31.4 mV (table 2 and Fig. 2). In contrast, formulation HP8-NP, which utilized a higher concentration of PEG, resulted in the largest particle size among the tested batches.

Table 1: Optimization involved varying drug/polymer ratios and polymer/surfactant combinations

Formulation	Polymer conc.	Surfactant conc.	Drug polymer ratio
HP1-NP	PEG: 0.25%	SLS: 0.5%	1:15
HP2-NP	PVP: 0.5%	SLS: 0.5%	1:15
HP3-NP	PVP: 0.25%	SLS: 0.5%	1:15
HP4-NP	HPMC: 0.25%	SLS: 0.5%	1:15
HP5-NP	EUD: 0.25%	SLS: 0.5%	1:15
HP6-NP	HPMC: 0.5%	SLS: 0.5%	1:10
HP7-NP	PVP: 0.5%	SLS: 0.5%	1:10
HP8-NP	PVP: 0.5%, HPMC: 0.5%	SLS: 0.5%	1:10
HP9-NP	PVP: 0.5%, HPMC: 0.5%	SLS: 0.5%	1:10
HP10-NP	PVP: 0.25%, HPMC: 0.25%	SLS: 1%	1:10
HP11-NP	PVP: 0.25%, HPMC: 0.25%	SLS: 0.5%	1:9
HP12-NP	PVP: 0.5%. HPMC: 0.5%	SLS: 1%	1:9
HP13-NP	HPMC: 0.5%	SLS: 1%	1:9
HP14-NP	HPMC: 0.25%	SLS: 1%	1:9
HP15-NP	PVP: 0.5%	SLS: 1%	1:9

Table 2: Physicochemical properties of optimized PQ-NP

S. No.	Parameter	Value (Mean ±SD)
1	Particle size (nm)	184±3.0
2	Polydispersity index (PDI)	0.248 ±0.012
3	Zeta potential (mV)	-31.4±1.3
4	Color	Somewhat white
5	Medling point	198.6 °C
6	Crystallinity	reduced crystallinity

Table 3: Pharmacokinetic parameters

Parameters	PQ-raw	PQ-NPs
C_{max} (µg/ml)	1.233 ± 0.2	2.753 ± 0.4
t_{max} (hr)	1.5 ± 0.3	1.0 ± 0.3
AUC (µg.hr/ml)	0.954 ± 0.01	1.119 ± 0.02

Stability of PQ-NPs at different temperatures

The physical stability of the PQ nanosuspensions was monitored over one month at 4°C and 25°C. Measurements of particle size, PDI, and zeta potential taken at intervals over 30 days showed that samples stored at 4°C maintained their initial characteristics with no significant changes (Fig. 3 and 4). The zeta potential also remained stable, indicating no substantial particle aggregation or instability throughout the study period.

Influence of temperature on zeta size of PQ-NPs

A one-month physical stability study was carried out on PQ nanosuspensions at two different temperatures, such as 4°C and 25°C, for the purpose of assessing the degree of particle growth and agglomeration. Over the period of one month, PDI and particle size quantification of the stored nanosuspensions were performed at designated intervals of time (0, 5, 10, 15, 20, 25, 30 days) using a Malvern Zeta Sizer. The particle size, PDI and zeta potential of PQ-NPs remained largely unchanged during 30 days of storage at 4°C (Figs. 3 and 4). Similarly, zeta potential values showed no significant shift, suggesting good colloidal stability. Although changes were minimal, these figures are included to visually confirm the absence of aggregation or instability over time.

Morphological Analysis by SEM

Scanning electron microscopy (SEM) revealed distinct morphological differences between the raw drug and the nanoparticles. The raw PQ appeared as large, elongated rods with smooth surfaces and sharp edges, consistent with a highly crystalline material (Fig. 5). Conversely, the optimized PQ-NP formulation (HP6-NP) consisted of spherical, submicron sized particles with a smooth surface and minimal aggregation (Fig. 6), aligning with the narrow size distribution observed in DLS.

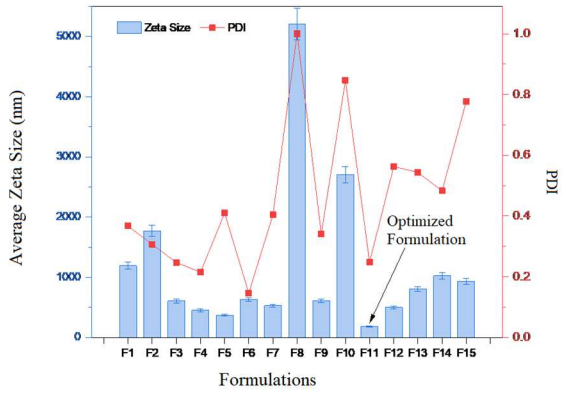

Fig. 1: Impact of various polymer combinations on particle size and PDI of PQ-NPs.

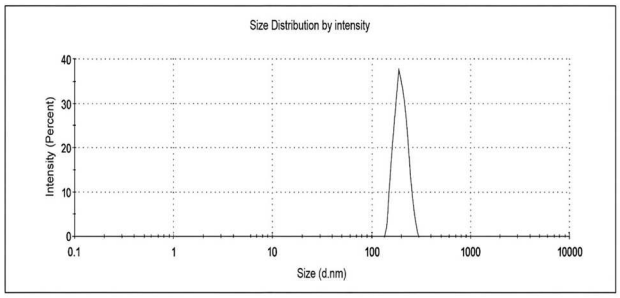

Fig. 2: Particle size analysis: Zeta size of PQ-NPs.

The SEM micrographs revealed that the anti-solvent precipitation technique yielded PQ-NPs with sizes in the submicron range, with an increased surface area and decreased nanoparticle size. The SEM image fig. 6 of the optimized formulation (HP6-NP) showed smooth, irregular nanoparticles with minimal aggregation. This correlates with the narrow size distribution and low PDI observed in DLS analysis. Formulations containing combinations of polymers and surfactants tended to produce smaller, more uniform particles, most likely due to their stabilization. In contrast, HPMC-based formulations exhibited slightly increased particle size due to higher viscosity during nano precipitation.

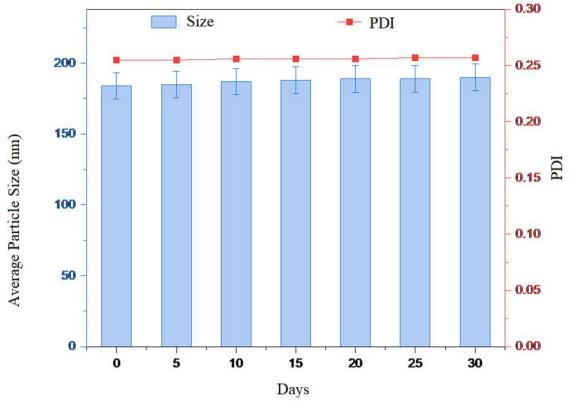

Fig. 3: Influence of temperature (4 °C) on size and PDI of PQ-NPs.

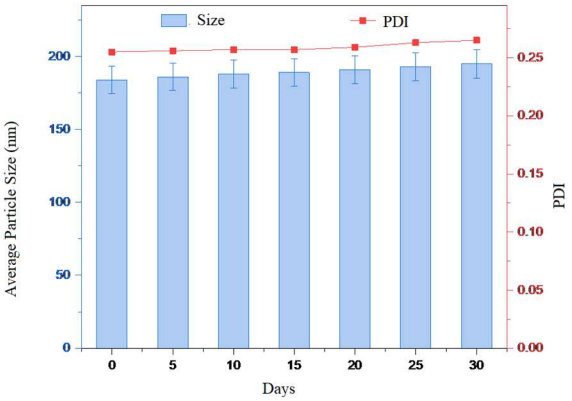

Fig. 4: Influence of temperature (25 °C) on size and PDI of PQ-NPs.

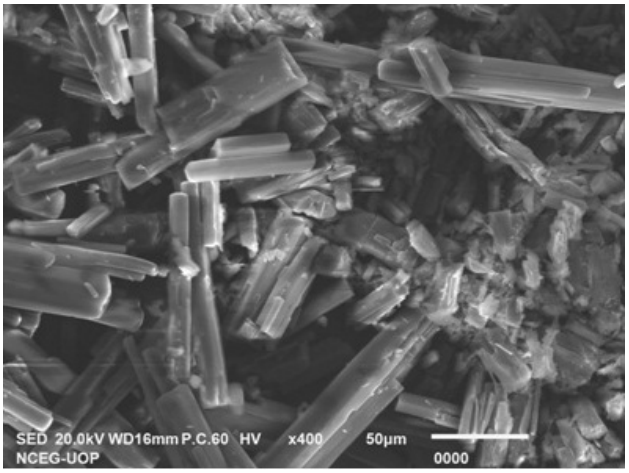

Fig. 5: SEM image of the raw PQ

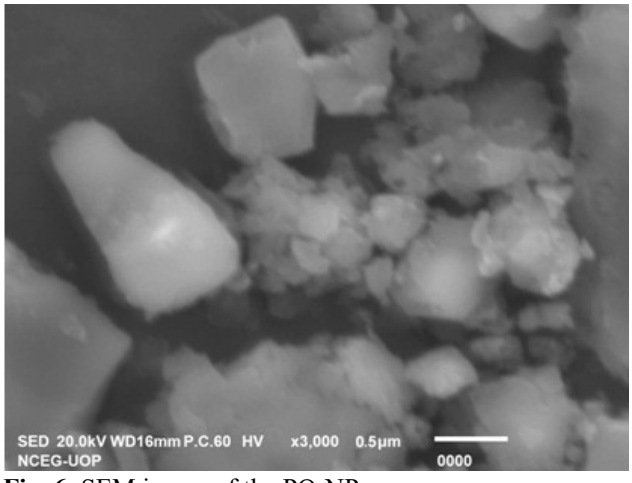

Fig. 6: SEM image of the PQ-NPs.

The XRD profile of the PQ-NPs was characterized by direct comparison with the XRD spectrum of the raw PQ, as shown in Fig. 7.

X-ray diffraction (XRD) analysis

The crystalline state of the raw drug and the nanoparticles was compared using XRD. The diffraction pattern of raw PQ showed numerous sharp, high-intensity peaks,

confirming its highly crystalline nature. The pattern for the PQ-NPs, however, displayed broader and less intense peaks, suggesting a reduction in crystallinity and a smaller crystallite size (Fig. 7).

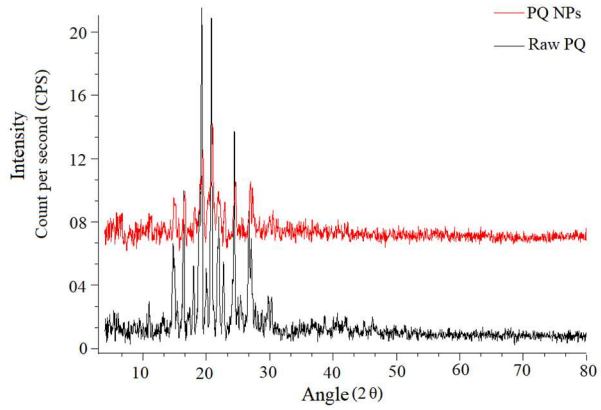

Fig. 7: XRD graph of the raw PQ and PQ-NPs.

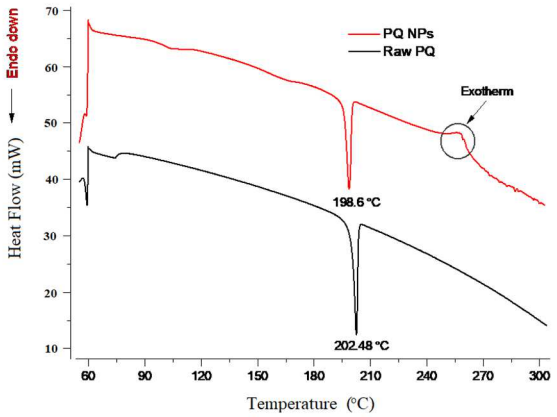

Fig. 8: DSC graph of the raw PQ and PQ-NPs

Differential scanning calorimetry (DSC)

The physical state of raw PQ and PQ-NPs has been evaluated using DSC and the resulting thermograms are presented in fig. 8. Both the raw PQ and the fabricated NPs exhibited a distinct melting endotherm, with a significant decrease in melting point observed for the nanocrystals compared to the raw PQ. The raw PQ revealed a melting point at 202.48°C. The melting point decreased to 198.6 °C upon precipitation as NPs. The reduction in melting point of PQ-NPs compared to raw PQ is due to the effects of reduced crystallinity.

Dissolution study

The *in-vitro* dissolution profiles of raw PQ and PQ-NPs are depicted in the fig. 9. PQ loaded NPs show a more rapid increase in drug release compared to the raw PQ. The PQ-NPs exhibit a markedly faster and more complete release profile, achieving nearly 79.56% drug release within 5 minutes compared to only about 27.31% for the raw PQ. The T-test indicated a significant difference of $P<0.05$ in the release of PQ from PQ-NPs in comparison with the raw PQ at a specific time point. The Noyes-Whitney equation demonstrates that the rate of dissolution of solids has a direct relation with their surface area when introduced to the dissolution medium.

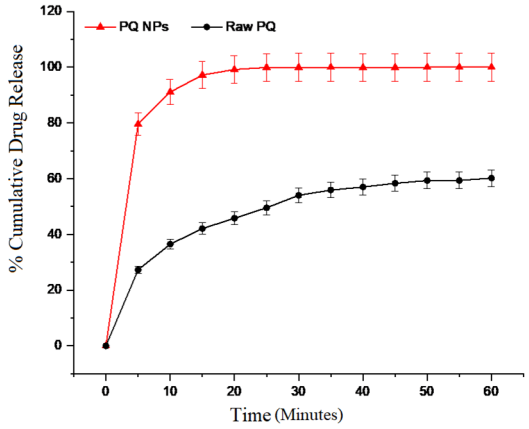

Fig. 9: Dissolution profile of raw PQ and PQ-NPs.

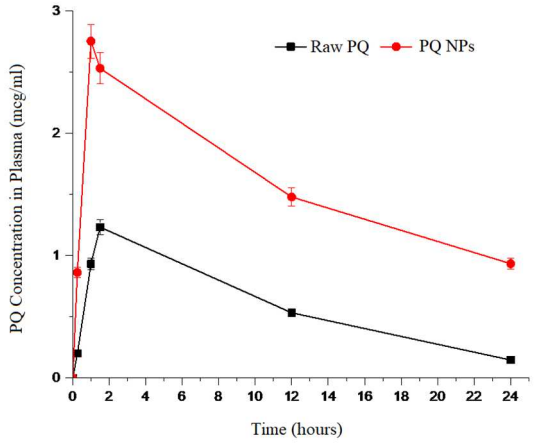

Fig. 10: Pharmacokinetic profile of Raw PQ and PQ-NPs.

Pharmacokinetic study

The concentration-time curve of raw PQ and PQ-NPs in plasma is shown in the fig.10. In the initial absorption phase, the concentration of PQ-NPs in plasma rises rapidly as compared to the raw PQ. Pharmacokinetic studies in mice revealed that $C_{max,}$ Tmax and AUC were significantly enhanced for PQ-NPs (C_{max}: 2.753 µg/ml vs. 1.233 µg/ml; Tmax: 1.0 ± 0.3 hr vs 1.5 ± 0.3 hr, AUC: 1.119 µg.hr/ml vs. 0.954 µg.hr/ml (Table3). These findings indicate the potential of PQ-NPs to enhance PQ therapeutic efficacy. These results indicate that the absorption and bioavailability of the formulations are based on nanoparticles.

DISCUSSION

The formulation screening identified a stabilizer system comprising HPMC, PVP-K30, and SLS as optimal for producing stable piperaquine nanocrystals. This

combination is effective in nanocrystal stabilization, as the polymers provide a steric barrier and ionic surfactants like SLS impart electrostatic repulsion, collectively preventing particle aggregation (Benamer Oudih *et al*., 2023; Inam *et al*., 2022). The increased particle size in formulation HP8-NP is likely a consequence of the higher PEG concentration, which can elevate system viscosity and hinder efficient nanoparticle formation (Al-Anssari *et al*., 2021, Tavakkoli *et al*., 2022) . The stability of nanocrystals is vital, as their high surface area confers significant surface free energy, predisposing them to instability (Tran *et al*., 2022). The consistent particle size, PDI, and zeta potential of the PQ-NPs stored at 4°C for one month confirm their strong stability and resistance to Ostwald ripening and aggregation (Lee and Fang, 2022). Morphological examination by SEM verified the successful production of submicron particles via anti-solvent precipitation. This reduction in particle size and the attendant increase in surface area are critical drivers for the observed enhancement in dissolution rate (Bilardo *et al*., 2022, Beach *et al*., 2024). The influence of polymer type on particle characteristics was evident; the steric stabilizer facilitated the formation of smaller, more uniform particles (Abdellatif *et al*., 2022, Khan *et al*., 2025), whereas the higher viscosity of HPMC solutions led to a slight increase in particle size (Miočić *et al*., 2025). The solid-state characterization techniques, XRD and DSC, provided compelling evidence of a change in the drug's physical form upon processing into nanoparticles. The XRD patterns indicated a notable decrease in crystallinity, a phenomenon known to improve drug solubility. The DSC results confirmed this finding, showing a lowered melting point for the PQ-NPs, which is characteristic of a less ordered crystalline structure or a partially amorphous state (Patel *et al*., 2021). This can be explained by the rapid nucleation during precipitation, which disrupts the perfect arrangement of molecules in the crystal lattice. The exothermic event at a higher temperature is likely a recrystallization phenomenon of the disordered drug upon heating (Shabatina *et al*., 2024). The enhanced dissolution rate of the PQ-NPs is a direct benefit of nanosizing, as described by the Noyes-Whitney equation, where a larger surface area accelerates dissolution (Gupta *et al*., 2021, Alhagiesa and Ghareeb, 2021). This *in-vitro* enhancement translated directly to *in-vivo* performance. The greater pharmacokinetic parameters, higher C_{max} and AUC, clearly demonstrate that the nanoformulation significantly improved the oral absorption and bioavailability of PQ (Liu *et al*., 2024). This confirms that formulating PQ as nanoparticles effectively overcomes its inherent solubility limited absorption, making the way for enhanced therapeutic efficacy.

CONCLUSION

PQ-NPs were successfully developed using anti-solvent precipitation technique, resulting in a significant reduction in particle size and increased surface area relative to the raw drug. The optimized formulations showed enhanced dissolution rates and improved drug solubility and exhibited favorable physicochemical characteristics, including good zeta potential and enhanced drug release behavior. Morphological analysis further confirmed uniform nanoscale dimensions, while DSC and XRD studies revealed reduced crystallinity and a shift toward an amorphous state, contributing to improved dissolution performance. Pharmacokinetic studies demonstrated a marked enhancement in oral bioavailability compared to pure PQ suspension. Collectively, these findings underscore the potential of PQ-NPs as a viable and effective strategy for improving the solubility, stability and therapeutic efficacy of PQ in oral drug delivery applications.

Acknowledgments
The authors are thankful to the Higher Education Commission of Pakistan and the Department of Pharmacy, University of Malakand

Authors' contributions
SB: Conducted the experimental work as a research scholar; J.K: Designed the study and provided supervision; MR: Supervision of the study and analysis of results; MAK, IT, HH and SA: Paper writing and critical revision of the article; AR and RG: Data analysis and interpretation of the results.

Funding
The authors are thankful to the Higher Education Commission of Pakistan for funding the NRPU Project No. 14913.

Data availability statement
The data is not publicly available due to privacy and ethical restrictions. The datasets generated during and/or analysed during the current study are available from the corresponding author on reasonable request.

Ethical approval
This study was conducted in accordance with ethical guidelines and approval was obtained from the ethical committee of the Department of Pharmacy, University of Malakand, with approval No REC/PHAR-UOM/2024/061. This study was performed in adherence with the ARRIVE guidelines. See supplementary file for the ARRIVE checklist.

Conflict of interest
On behalf of all authors, the corresponding author states that there is no conflict of interest.

Supplementary data
https://www.pjps.pk/uploads/2026/04/SUP1775907627.pdf

REFERENCES

Abdellatif AA, Tolba NS, Alsharidah M, Al Rugaie O, Bouazzaoui A, Saleem I, Maswadeh H and Ali AT (2022). PEG-4000 formed polymeric nanoparticles loaded with cetuximab downregulate p21 and stathmin-1 gene expression in cancer cell lines. *Life Sci.*, **295**(1): 120403.

Al-Anssari S, Ali M, Alajmi M, Akhondzadeh H, Khaksar Manshad A, Kalantariasl A, Iglauer S and Keshavarz A (2021). Synergistic effect of nanoparticles and polymers on the rheological properties of injection fluids: Implications for enhanced oil recovery. *Energy Fuels*, **35**(8): 6125-6135.

Alhagiesa AW and Ghareeb MM (2021). The formulation and characterization of nimodipine nanoparticles for the enhancement of solubility and dissolution rate. *Iraqi J. Pharm. Sci.*, **30**(1): 143-152.

Alqahtani MS, Kazi M, Alsenaidy MA and Ahmad MZ (2021). Advances in oral drug delivery. *Front. Pharmacol.*, **12**(1): 618411.

Beach MA, Nayanathara U, Gao Y, Zhang C, Xiong Y, Wang Y and Such GK (2024). Polymeric nanoparticles for drug delivery. *Chem. Rev.*, **124**(10): 5505–5616.

Benamer Oudih S, Tahtat D, Nacer Khodja A, Mahlous M, Hammache Y, Guittoum AE and Kebbouche Gana S (2023). Chitosan nanoparticles with controlled size and zeta potential. *Polym. Eng. Sci.*, **63**(4): 1011-1021.

Bhalani DV, Nutan B, Kumar A and Singh Chandel AK (2022). Bioavailability enhancement techniques for poorly aqueous soluble drugs and therapeutics. *Biomedicines*, **10**(9): 2055.

Bilardo R, Traldi F, Vdovchenko A and Resmini M (2022). Influence of surface chemistry and morphology of nanoparticles on protein corona formation. *Wiley Interdiscip. Rev. Nanomed. Nanobiotechnol.*, **14**(4): e1788.

Boscolo O, Flor S, Salvo L, Dobrecky C, Hocht C, Tripodi V, Moretton M and Lucangioli S (2023). Formulation and characterization of ursodeoxycholic acid nanosuspension based on bottom-up technology and Box-Behnken design optimization. *Pharmaceutics*, **15**(1): 1-15.

Da Silva FLO, Marques MBF, Kato KC and Carneiro G (2020). Nanonization techniques to overcome poor water-solubility with drugs. *Expert Opin. Drug Discov.*, **15**(7): 853-864.

Dolatabadi S, Karimi M, Nasirizadeh S, Hatamipour M, Golmohammadzadeh S and Jaafari MR (2021). Preparation, characterization and *in vivo* pharmacokinetic evaluation of curcuminoids-loaded solid lipid nanoparticles (SLNs) and nanostructured lipid carriers (NLCs). *J. Drug Deliv. Sci. Technol.*, **62**(1): 102352.

Fonte M, Tassi N, Gomes P and Teixeira C (2021). Acridine-based antimalarials—from the very first synthetic antimalarial to recent developments. *Molecules*, **26**(3): 600.

Ghanbari E, Picken SJ and Van Esch JH (2023). Analysis of differential scanning calorimetry (DSC): Determining the transition temperatures and enthalpy and heat capacity changes in multicomponent systems by analytical model fitting. *J. Therm. Anal. Calorim.*, **148**(20): 12393-12409.

Graván P, Aguilera-Garrido A, Marchal JA, Navarro-Marchal SA and Galisteo-González F (2023). Lipid-core nanoparticles: Classification, preparation methods, routes of administration and recent advances in cancer treatment. *Adv. Colloid Interface Sci.*, **314**(1): 102871.

Gupta R, Chen Y and Xie H (2021). In vitro dissolution considerations associated with nano drug delivery systems. *Wiley Interdiscip. Rev. Nanomed. Nanobiotechnol.*, **13**(5): e1732.

Hami Z (2021). A brief review on advantages of nano-based drug delivery systems. *Ann. Mil. Health Sci. Res.*, **19**(2): 1-6.

Haripriyaa M and Suthindhiran K (2023). Pharmacokinetics of nanoparticles: current knowledge, future directions and its implications in drug delivery. *Future J. Pharm. Sci.*, **9**(1): 113.

Hung TY, Davis TM and Ilett KF (2003). Measurement of piperaquine in plasma by liquid chromatography with ultraviolet absorbance detection. *J. Chromatogr. B*, **791**(1-2): 93-101.

Inam W, Bhadane R, Akpolat RN, Taiseer RA, Filippov SK, Salo-Ahen OM, Rosenholm JM and Zhang H (2022). Interactions between polymeric nanoparticles and different buffers as investigated by zeta potential measurements and molecular dynamics simulations. *VIEW*, **3**(1): 20210009.

Khan S, Nawaz A, Shah MKA, Latif MS, Haroon M, Khan A and Elsayed TMA (2025). Formulation and characterization of isavuconazole-loaded chitosan/ sodium alginate nanoparticles for dermal delivery: *In vitro* and *in vivo* evaluation for enhanced antifungal therapy. *J. Pharm. Innov.*, **20**(1): 156.

Khan ZU, Razzaq A, Khan A, Rehman NU, Khan H, Khan T, Khan AU, Althobaiti NA, Menaa F and Iqbal H (2022). Physicochemical characterizations and pharmacokinetic evaluation of pentazocine solid lipid nanoparticles against inflammatory pain model. *Pharmaceutics*, **14**(2): 409.

Kumar R, Dalvi SV and Siril PF (2020). Nanoparticle-based drugs and formulations: Current status and emerging applications. *ACS Appl. Nano Mater.*, **3**(6): 4944-4961.

Kumar R, Thakur AK, Kali G, Pitchaiah KC, Arya RK and Kulabhi A (2023). Particle preparation of pharmaceutical compounds using supercritical antisolvent process: current status and future perspectives. *Drug Deliv. Transl. Res.*, **13**(3): 946-965.

Lee CH and Fang JKH (2022). Effects of temperature and particle concentration on aggregation of nanoplastics in

freshwater and seawater. *Sci. Total Environ.*, **817**(1): 152562.

Liu Y, Liang Y, Yuhong J, Xin P, Han JL, Du Y, Yu X, Zhu R, Zhang M and Chen W (2024). Advances in nanotechnology for enhancing the solubility and bioavailability of poorly soluble drugs. *Drug Des. Dev. Ther.*, **18**(1): 1469-1495.

Lou J, Duan H, Qin Q, Teng Z, Gan F, Zhou X and Zhou X (2023). Advances in oral drug delivery systems: Challenges and opportunities. *Pharmaceutics*, **15**(2): 484.

Mahmood T, Sarfraz RM, Ismail A, Ali M and Khan AR (2023). Pharmaceutical methods for enhancing the dissolution of poorly water-soluble drugs. *ASSAY Drug Dev. Technol.*, **21**(2): 65-79.

Miočić S, Torić J, Juretić M, Đoković J, Randjelović D, Savić S, Ferderber K, Čižmek BC and Filipović-Grčić J (2025). Characterisation and stabilisation mechanisms of azelaic acid nanosuspensions: Insights from a dual stabiliser system. *Pharmaceutics*, **17**(3): 439.

Mitchell MJ, Billingsley MM, Haley RM, Wechsler ME, Peppas NA and Langer R (2021). Engineering precision nanoparticles for drug delivery. *Nat. Rev. Drug Discov.*, **20**(2): 101-124.

Mollaeva MR, Yabbarov N, Sokol M, Chirkina M, Mollaev MD, Zabolotskii A, Seregina I, Bolshov M, Kaplun A and Nikolskaya E (2021). Optimization, characterization and pharmacokinetic study of meso-tetraphenylporphyrin metal complex-loaded PLGA nanoparticles. *Int. J. Mol. Sci.*, **22**(22): 12261.

Niroumand U, Firouzabadi N, Goshtasbi G, Hassani B, Ghasemiyeh P and Mohammadi-Samani S (2023). The effect of size, morphology and surface properties of mesoporous silica nanoparticles on pharmacokinetic aspects and potential toxicity concerns. *Front. Mater.*, **10**(1): 1189463.

Pandita D, Munjal A, Poonia N, Awasthi R, Kalonia H and Lather V (2021). Albumin-coated mesoporous silica nanoparticles of docetaxel: Preparation, characterization and pharmacokinetic evaluation. *ASSAY Drug Dev. Technol.*, **19**(4): 226-236.

Parida S, Bal U, Mahapatra AK and Swain S (2024). Biopharmaceutics classification system (BCS) and biowaiver in drug product design. *Res. J. Pharm. Life Sci.*, **5**(1): 11-28.

Patel B, Tripathi SK, Shukla S and Pandey A (2021). Preparation, characterisation and *in vitro* drug release study of chloroquine phosphate-loaded chitosan nanoparticles as malaria treatment. *Oxid. Commun.*, **44**(1): 1–10.

Ran Q, Wang M, Kuang W, Ouyang J, Han D, Gao Z and Gong J (2022). Advances of combinative nanocrystal preparation technology for improving the insoluble drug solubility and bioavailability. *Crystals*, **12**(9): 1-16.

Sabra R, Kirby D, Chouk V, Malgorzata K and Mohammed AR (2024). Buccal absorption of biopharmaceutics classification system III drugs: Formulation approaches and mechanistic insights. *Pharmaceutics*, **16**(11): 1563.

Shabatina TI, Gromova YA, Vernaya OI, Soloviev AV, Shabatin AV, Morosov YN, Astashova IV and Melnikov MY (2024). Pharmaceutical nanoparticles formation and their physico-chemical and biomedical properties. *Pharmaceuticals*, **17**(4): 587.

Sharma B, Agarwal A and Awasthi SK (2023). Is structural hybridization invoking new dimensions for antimalarial drug discovery research? *RSC Med. Chem.*, **14**(6): 1227-1253.

Song Y, Feng L, Zhong W, Tripathi S, Ananthoji PK, Armenante P and Sirkar KK (2025). Porous hollow fiber membrane-based continuous cross-flow anti-solvent crystallizer for production of API nanocrystals. *Sep. Purif. Technol.*, **350**(1): 134331.

Tavakkoli O, Kamyab H, Shariati M, Mohamed AM and Junin R (2022). Effect of nanoparticles on the performance of polymer/surfactant flooding for enhanced oil recovery: A review. *Fuel*, **312**(1): 122867.

Tran T, Perdomo MEG, Haghighi M and Amrouch K (2022). Study of the synergistic effects between different surfactant types and silica nanoparticles on the stability of liquid foams at elevated temperature. *Fuel*, **315**(1): 122818.

Urimi D, Widenbring R, García ROP, Gedda L, Edwards K, Loftsson T and Schipper N (2021). Formulation development and upscaling of lipid nanocapsules as a drug delivery system for a novel cyclic GMP analogue intended for retinal drug delivery. *Int. J. Pharm.*, **602**(1): 120640.

Yadav D and Kumar N (2014). Nanonization of curcumin by antisolvent precipitation: Process development, characterization, freeze drying and stability performance. *Int. J. Pharm.*, **477**(1-2): 564-577.

Zhang X, Li Q, Wang J, Huang J, Huang W and Huang Y (2024). Physicochemical properties and *in vitro* release of formononetin nanoparticles by ultrasonic probe-assisted precipitation in four polar organic solvents. *Food Chem.*, **461**(1): 140918.

Zulbeari N and Holm R (2025). Long-term versus short-term stress physical stability assessment of pharmaceutical nano- and microsuspensions. *Int. J. Pharm.*, **655**(1): 125646.